Fabrication and Characterization of Metal−Molecule−Metal Junctions by Conducting Probe Atomic Force Microscopy

David J. Wold and C. Daniel Frisbie*

Contribution from the Department of Chemical Engineering and Materials Science, University of Minnesota, 421 Washington Avenue SE, Minneapolis, Minnesota 55455

Received January 17, 2001

Abstract: Metal−molecule−metal junctions were fabricated by contacting Au-supported alkyl or benzyl thiol self-assembled monolayers (SAMs) with an Au-coated atomic force microscope (AFM) tip. The tip−SAM microcontact is approximately 15 nm^2, meaning the junction contains ∼75 molecules. Current−voltage ($I-V$) characteristics of these junctions were probed as a function of SAM thickness and load applied to the microcontact. The measurements showed: (1) the $I-V$ traces were linear over ±0.3 V, (2) the junction resistance increased exponentially with alkyl chain length, (3) the junction resistance decreased with increasing load and showed two distinct power law scaling regimes, (4) resistances were a factor of 10 lower for junctions based on benzyl thiol SAMs compared to hexyl thiol SAMs having the same thickness, and (5) the junctions sustained fields up to 2×10^7 V/cm before breakdown. $I-V$ characteristics determined for bilayer junctions involving alkane thiol-coated tips in contact with alkane thiol SAMs on Au also showed linear $I-V$s over ±0.3 V and the same exponential dependence on thickness. The $I-V$ behavior and the exponential dependence of resistance on alkyl chain length are consistent with coherent, nonresonant electron tunneling across the SAM. The calculated conductance decay constant (β) is 1.2 per methylene unit (∼1.1 Å^{-1}) for both monolayer and bilayer junctions, in keeping with previous scanning tunneling microscope and electrochemical measurements of electron transfer through SAMs. These measurements show that conducting probe-AFM is a reliable method for fundamental studies of electron transfer through small numbers of molecules. The ability to vary the load on the microcontact is a unique characteristic of these junctions and opens opportunities for exploring electron transfer as a function of molecular deformation.

Introduction

Metal−molecule−metal junctions (m−M−m) are useful devices for exploring the structural and electronic factors affecting electrical transport in molecules. In these junctions, individual molecules or molecular assemblies are contacted by two metal electrodes, as shown in Scheme 1A. The junction conductance depends on a wide spectrum of factors including molecular dimensions (i.e., the distance between the electrodes), the molecular HOMO−LUMO energy gap, the molecular ionization potential, the metal work function, the molecular bonding and functional group architectures, and contact properties.[1−4] While these factors are generally appreciated, quantitative understanding of the current−voltage ($I-V$) characteristics of these junctions is just beginning to emerge. Metal−molecule−metal junctions are currently being considered as key elements in molecule-based electronic devices,[5] providing clear motivation for investigating their properties. It is also anticipated that detailed studies of these junctions will augment fundamental understanding of molecular electron-transport processes, central to many aspects of chemistry.[6] In this sense, transport studies

Scheme 1. (A) Metal−Molecule−Metal Junction and (B) Electrostatic Potential Profile across a Junction[a]

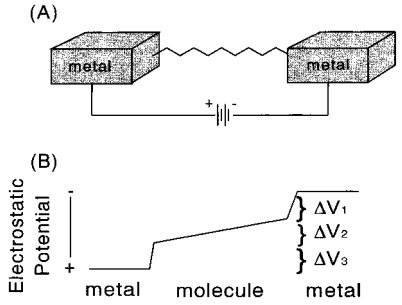

[a] ΔV_1 and ΔV_3 are the voltage drops at the contacts. ΔV_2 is the voltage drop across the molecule.

* Address correspondence to this author. E-mail: frisbie@cems.umn.edu.

(1) (a) Segal, D.; Nitzan, A.; Davis, W. B.; Wasielewski, M. R.; Ratner, M. A. *J. Phys. Chem. B* **2000**, 104, 3817−3829. (b) Mujica, V.; Roitberg, A. E.; Ratner, M. *J. Chem. Phys*. **2000**, 112, 6834−6839. (c) Yaliraki, S. N.; Kemp, M.; Ratner, M. A. *J. Am. Chem. Soc*. **1999**, *121*, 3428. (d) Yalikari, S. N.; Roitberg, A. E.; Gonzalez, C.; Mujica, V.; Ratner, M. *J. Chem. Phys*. **1999**, 111, 6997−7002. (e) Ratner, M. A.; Davis, B.; Kemp, M.; Mujica, V.; Roitberg, A.; Yaliraki, S. *Ann. N.Y. Acad. Sci.*, **1998**, 852. (f) Kemp M.; Roitberg, A.; Mujica, V.; Wanta, T.; Ratner, M. *J. Phys. Chem.* **1996**, 100, 8349−8355.

(2) (a) Datta, S.; Tain, W.; Hong, S.; Reifenberger, R.; Henderson, J. I.; Kubiak, C. P. *Phys. Rev. Lett*. **1997**, 79, 2530−2533. (b) Samanta, M. P.; Tian, W.; Datta, S.; Henderson, J. I.; Kubiak, C. P. *Phys. Rev. B* **1996**, 53, R7626−R7629.

(3) (a) Magoga, M.; Joachim, C. *Phys. Rev. B* **1999**, 59, 16011−16021. (b) Magoga, M.; Joachim, C. *Phys. Rev. B* **1997**, 56, 4722−4729. (c) Joachim, C.; Vinuesa, J. F. *Europhys. Lett*. **1996**, 33, 635−640.

(4) Onipko, A. *Phys. Rev. B* **1999**, 59, 9995−10006.

(5) (a) Tour, J. M.; *Acc. Chem. Res.* **2000**, 33, 791−804. (b) Reed, M. A.; Tour, J. M. *Sci. Am.* **2000**, 282, 86−93. (c) Heath, J. R. *Pure Appl. Chem*. **2000**, 72, 11−20. (d) Rueckes, T.; Kim, K.; Joselevich, E.; Tsen, G. Y.; Cheung, C.-L.; Lieber, C. M. *Science* **2000**, 289 (5476), 94−97.

(6) (a) Ratner, M. *Nature* **2000**, 404(6774), 137−138. (b) Jortner, J.; Ratner, M. *Molecular Electronics;* Blackwell, London, 1997. (b) Winkler, J. R.; DiBilio, A. J. Furrow, N. A.; Richards, J. H.; Gray, H. B. *Pure Appl. Chem*. **1999**, 71, 1753−1764. (c) Marcus, R. A. *Pure Appl. Chem*. **1997**, 69, 13−29. (d) Tolbert, L. *Acc. Chem. Res*. **1992**, 25, 561−568.

10.1021/ja0101532 CCC: $20.00
Published on Web 05/18/2001

of these junctions are complementary to the vast number of spectroscopic,[7] electrochemical,[8] and scanning tunneling microscopy (STM)[9] investigations of inter- and intramolecular electron transfer.

Strategies for fabricating metal−molecule−metal junctions include assembling molecules inside metal-capped nanopores[10] and mechanical break junctions[11] or between mercury drops,[12] nanofabricated electrodes,[13] and crossed wires.[14] Metallic nanoparticles have also been used as electrical contacts to molecular monolayers supported on metal surfaces.[15] Theoretical investigations of the transport properties of metal−molecule−metal junctions are being pursued by several research groups.[1−4]

We have recently described an alternative approach to the formation of metal−molecule−metal junctions using conducting probe atomic force microscopy (CP-AFM).[16] A junction is fabricated by placing a conducting AFM tip in contact with a metal−supported molecular film, such as a self-assembled monolayer (SAM) on Au, as shown in Scheme 2A. The normal force feedback circuit of the AFM controls the mechanical load on the microcontact while the current−voltage ($I-V$) characteristics are recorded. The ability to manipulate the load on the microcontact is an unusual characteristic of this type of junction and provides the opportunity to probe the relationship between mechanical deformation of molecules and their transport properties. Additionally, the load-dependent tip−SAM contact area in these junctions is small (of order 10 nm^2), meaning the junction properties reflect transport through a small number of molecules, typically less than 100 for a 50 nm radius probe.

Scheme 2. Formation of Monolayer (A) and Bilayer (B) Junctions Using a Au-Coated AFM Tip[a]

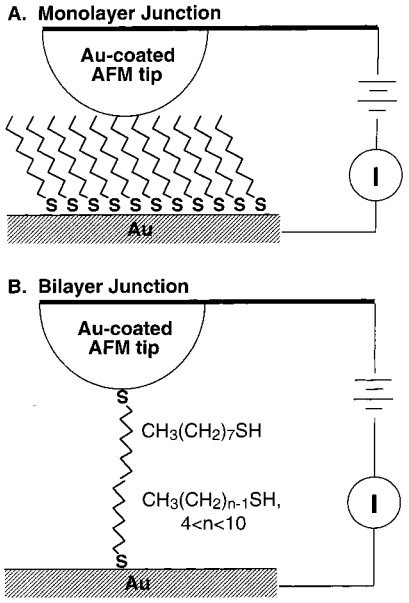

[a] For the bilayer junctions, the tip was coated with a $CH_3(CH_2)_7SH$ SAM and the thickness of the SAM on the substrate was varied as indicated. For both monolayer and bilayer junctions, voltages were applied to the probe tip; the substrate was grounded.

A key advantage of CP-AFM for junction fabrication is that no micro- or nanofabrication processes are necessary. This means that, in terms of time, screening of junction behavior is limited by synthesis of molecules and their assembly on conducting substrates, and not by the measurement methodology itself. The Hg drop junctions reported by Rampi and Whitesides share this characteristic.[12a−c] Junction fabrication by CP-AFM is also a "soft" process in that there are no high-temperature contact-forming steps. Molecules may be contacted by any conducting film that can be coated onto an AFM tip, offering flexibility for examining the role of contacts on the junction $I-V$ behavior.

It is important to note the difference between this CP-AFM method and scanning tunneling microscopy (STM) for characterizing molecular junctions. In STM, current, not force, is used to control tip-positioning. Because the conductance properties of molecules are generally unknown, the position of the probe with respect to the molecules can be ambiguous. If the STM tip is not in contact with the monolayer, the junction transport properties are determined by the molecules *and the vacuum (or air) gap* between the molecules and the tip. If the tip penetrates the monolayer, it is difficult to know how far it has penetrated and thus what portions of the molecules contribute to the current. CP-AFM does not have this difficulty because an independent feedback signal, namely normal force, allows the probe to be controllably positioned just in contact with the monolayer. At

(7) (a) Davis, W. B.; Svec, W. A.; Ratner, M. A.; Wasielewski, M. R. *Nature* **1998**, 396(6706), 60−63. (b) Arkin, M. R.; Stemp, E. D. A.; Holmlin, R. E.; Barton, J. K.; Hormann, A.; Olson, E. J.; Barbara, P. F. *Science* **1996**, 273(5274), 457−480.

(8) (a) Slowinski, K.; Slowinska, K.; Majda, M. *J. Phys. Chem. B* **1999**, 105, 8544−8551. (b) Delville, M.; Tsionsky, M.; Bard, A. *Langmuir* **1998**, 14, 2774−2779. (c) Sachs, S. B.; Dudek, S. P.; Hsung, R. P.; Sita, L. R.; Smalley, J. F.; Newton, M. D.; Feldberg, S. W.; Chidsey, C. E. D. *J. Am. Chem. Soc.* **1997**, 119, 10563−10564. (d) Slowinski, K.; Chamberlain, R. V.; Miller, C. J.; Majda, M. *J. Am. Chem. Soc.* **1997**, 119, 11910−11919. (e) Smalley, J. F.; Feldberg, S. W.; Chidsey, C. E. D.; Linford, M. R.; Newton, M. D.; Liu, Y. *J. Phys. Chem.* **1995**, 99, 13141−13149. (f) Ravenscroft, M. S.; Finklea, H. O. *J. Phys. Chem.* **1994**, 98, 3843−3850. (g) Forster, R. J.; Faulkner, L. R. *J. Am. Chem. Soc.* **1994**, 116, 5453−5461. (h) Chidsey, C. E. D. *Science* **1991**, 251, 919−922.

(9) (a) Bumm, L. A.; Arnold, J. J.; Dunbar, T. D.; Allara, D. L., Weiss, P. S. *J. Phys. Chem. B* **1999**, 103, 8122−8127. (b) Xue, Y.; Datta, S.; Hong, S.; Reifenberger, R.; Henderson, J.; Kubiak, C. *Phys. Rev. B* **1999**, 59, R7852−R7855. (c) Tian, W.; Datta, S.; Hong, S.; Reifenberger, R.; Henderson, J.; Kubiak, C. *J. Chem. Phys.* **1998**, 109, 2874−2882. (d) Datta, S.; Tian, W.; Hong, S.; Reifenberger, R.; Henderson, J.; Kubiak, C. *Phys. Rev. Lett.* **1997**, 79, 2530−2533. (e) Magoga, M.; Joachim, C. *Phys. Rev. B.* **1997**, 56, 4722−4729. (f) Dhirani, A.; Lin, P. H.; Guyot-Sionnest, P.; Zehner, R. W.; Sita, L. R. *J. Chem. Phys.* **1997**, 106, 5249−5253. (g) Bumm, L. A.; Arnold, J. J.; Cygan, M. T.; Dunbar, T. D.; Burgin, T. P.; Jones, L., II; Allara, D. L.; Tour, J. M.; Weiss, P. S. *Science* **1996**, 271, 1705−1707. (h) Joachim, C.; Gimzewski, J. K.; Schlitter, R. R.; Chavy, C. *Phys. Rev. Lett.* **1995**, 74, 2102−2105.

(10) (a) Chen, J.; Reed, M. A.; Rawlett, A. M.; Tour, J. M. *Science* **1999**, 286, 1550−1552. (b) Zhou, C.; Deshpande, M. R.; Reed, M. A.; Jones, L., II; Tour, J. M. *Appl. Phys. Lett.* **1997**, 71, 611−613.

(11) (a) Reed, M. A.; Zhou, C.; Muller, C. J.; Burgin, T. P.; Tour, J. M. *Science* **1997**, 278, 252−254. (b) Kergueris, Bourgoin, J.-P.; Palacin, S.; Esteve, D.; Urbina, C.; Magoga, A.; Joachim, C. *Phys. Rev. B* **1999**, 59, 12505−12513.

(12) (a) Holmlin, R. E.; Haag, R.; Chabinyc, M. L.; Ismagilov, R. F.; Cohen, A. E.; Terfort, A. E.; Rampi, M. A.; Whitesides, G. M. *J. Am. Chem. Soc*. Manuscript submitted. (b) Haag, R.; Rampi, M. A.; Holmlin, R. E.; Whitesides, G. M. *J. Am. Chem. Soc.* **1999**, 121, 7895−7906. (c) Rampi, M. A.; Schueller, O. J. A.; Whitesides, G. M. *Appl. Phys. Lett.* **1998**, 72, 1781−1783. (d) Slowinski, K.; Fong, H. K. Y.; Majda, M. *J. Am. Chem. Soc.* **1999**, *121*, 7257−7261.

(13) (a) Park, H.; Park, J.; Lim, A. K.; Anderson, E. N.; Alivisatos, A. P.; McEuen, P. L. *Nature* **2000**, 407(6800), 58−60. (b) Tans, S. J.; Verschueren, A. R. M.; Dekker, C. *Nature* **1998**, 393, 49−52.

(14) (a) Wong, E. W.; Collier, C. P.; Beloradsky, M.; Raymor, F. M.; Stoddart, J. F.; Heath, J. R. *J. Am. Chem. Soc*. **2000**, 122, 5831. (b) Metzger, R. M. *Acc. Chem. Res.* **1999**, 32, 950−957. (c) Collier, C. P.; Wong, E. W.; Beloradsky, M.; Raymo, F. M.; Stoddard, J. F.; Kuekes, P. J.; Williams, R. S.; Heath, J. R. *Science* **1999**, 285, 391−394. (d) Metzger, R. M.; Chen, B.; Hopfner, U.; Lakshmikantham, M. V.; Vuillaume, D.; Kawai, T.; Wu, X.; Tachibana, H.; Hughes, T. V.; Sakurai, H.; Baldwin, J. W.; Hosch, C.; Cava, M. P.; Brehmer, L.; Ashwell, G. J. *J. Am. Chem. Soc.* **1997**, 119, 10455−10466. (e) Fischer, C. M.; Burghard, M.; Roth, S.; von Klitzing, K. *Surface Science* **1996**, 362, 905−908.

(15) Dorogi, M.; Gomez, J.; Osifchin, R.; Andres, R. P.; Reifenberger, R. *Phys. Rev. B* **1995**, 52, 9071−9077.

(16) Wold, D. J.; Frisbie, C. D. *J. Am. Chem. Soc.* **2000**, 122, 2970−2971.

low contact forces, there is much less ambiguity in CP-AFM about where the tip is with respect to the endgroups of the SAM.

Previous CP-AFM studies of electrical transport in molecules include resistance measurements along carbon nanotubes[17] and $I-V$ measurements across Langmuir−Blodgett films[18] and adsorbed alkane layers.[19] Lindsay and co-workers used Pt-coated AFM tips to generate two-dimensional "current maps" of docosane thiol SAMs with imbedded β-carotene derivatives.[20] By analyzing the bright spots in these images as a function of applied tip−substrate bias, they estimated the resistance of the β-carotene molecule to be 4 GΩ. Salmeron, et al. measured current and cantilever deflection simultaneously as a lever was brought into contact with a SAM of $CH_3(CH_2)_{11}SH$.[21] Our initial study demonstrated that the $I-V$ characteristics of SAMs could be recorded using a stationary, conducting tip under fixed applied load.[16]

Transport through metal−molecule−metal junctions is expected to depend critically on the properties of the contacts, which in turn depend on the details of the chemisorption or physisorption at the metal−molecule interfaces. The influence of the contacts can be described by the electrostatic potential profile across the junction. Datta has concluded that to first approximation the change in potential is not linear, but instead displays sharp drops at the electrode−molecule interfaces,[2] as shown in Scheme 1B. Equal potential drops at both contacts were necessary to account for symmetric $I-V$ characteristics observed in STM conductance studies of SAMs. A recent self-consistent solution of the Schrödinger and Poisson equations for a metal−molecule−metal junction by Mujica et al.[1b] supports Datta's original conclusion that the profile has the general shape shown in Scheme 1B. A density functional theory (DFT) calculation by Lang and Avouris of the electrostatics for a metal−cumulene−metal junction tells a slightly different story;[22] there are no steep changes in the potential profile, but a large fraction of the total potential is dropped just *inside* the metallic contacts. In either case, the upshot is that a large fraction of the applied potential is dropped at (or within) the contacts, meaning that the contacts represent a significant bottleneck to current flow. To determine the resistance of the molecular bridge, it is therefore necessary to account for the voltage drop (effective resistance) at the contacts. This can be done by measuring the junction resistance as a function of electrode spacing (molecular length), which yields the resistance per unit length of molecule, a quantity that is independent of the contact properties.

The length dependence of the junction resistance hinges on the transport mechanism through the junction, and in principle can fall into one of three categories, coherent resonant tunneling, coherent nonresonant tunneling, and diffusive (noncoherent) transport, as described by Ratner.[1e] When the Fermi level of the junction lies within the HOMO−LUMO gap of the molecules, the transport mechanism is expected to be coherent nonresonant tunneling (analogous to "super-exchange" in molecular electron-transfer theory). In this regime, the junction resistance scales exponentially with the electrode separation, which is proportional to molecular length. The resistance for the junction is expressed as

$$R = R_0 \exp(\beta s) \quad (1)$$

where R_0 is an effective contact resistance, s is the junction length, and the exponential prefactor β, with units of 1/length, is a structure-dependent measure of transport efficiency.

In our initial work demonstrating the fabrication of metal−molecule−metal junctions by CP-AFM,[16] we showed that the resistance of junctions formed with alkane thiol SAMs (Scheme 2A) increased exponentially with alkane chain length. The exponential dependence is consistent with coherent nonresonant electron tunneling, although the prefactor β we determined (1.45 $Å^{-1}$) was somewhat higher than β values obtained by other methods (e.g., 1.0 $Å^{-1}$ by electrochemical techniques[8e]). In this paper, we describe a more complete set of experiments in which we have investigated the effects of the applied microcontact load, tip radius, voltage sweep range, and tip chemical modification on the ($I-V$) response of Au−alkane thiol−Au junctions. We find that the breakdown voltage of this junction scales with SAM thickness in a fashion similar to recently reported Hg contact junctions.[12b] We also show that the junction resistance has two distinct regimes of power law dependence on load, and that bilayer junctions may be probed, opening the possibility of determining the role of functional group interactions on β. Finally, we have repeated the length dependence study using a broader range of alkane thiol chain lengths and slightly lower microcontact load. We find that the new β value (1.1 $Å^{-1}$) is closer to previously reported values. Our measurements establish that CP-AFM is a useful method for characterizing electron transport through molecules.

Experimental Section

Materials. Gold wire (99.999% pure) was purchased from Mowrey, Inc. (St. Paul, MN). Cr was purchased from R.D. Mathis (Long Beach, CA). Ethanol (200 proof) was used as received from Quantum (Newark, NJ). Benzylthiol and all alkane thiols were used as purchased from Aldrich.

Monolayer Preparation. Gold films were deposited onto Si substrates using a thermal evaporator at a background pressure of 3×10^{-6} Torr. Typically, 400 Å of gold was deposited on a 30 Å Cr adhesion layer at 1 Å/s. Immediately after metallization, the Au-coated Si was cleaved into 1 cm^2 chips and placed into freshly prepared 1 mM thiol solutions in ethanol. A monolayer was allowed to form for at least 12 h (usually overnight). Before use, each sample was rinsed with several mL of absolute ethanol and gently blown dry with N_2.

Junction Formation and Characterization. Unless otherwise noted, all measurements were made using a Digital Instruments MultiMode AFM (Santa Barbara, CA) with commercially available V-shaped Si_3N_4 cantilevers (nominal force constant 0.06 N/m). Fresh tips were metallized weekly as above with a 40 nm gold film and stored at atmosphere until use.

Junctions were formed by placing the conducting tips in stationary point contact, under controlled load, with the SAM surface. The mechanical load was held constant using standard AFM feedback. The $I-V$s were recorded using a Keithley 236 source measure unit controlled by a computer running LabView software. Voltages were applied to the tip; the Au/SAM substrate was grounded. Typically, $I-V$s were recorded as a function of load at five different points on the sample surface to ensure repeatability. The tips were not scanned over the surface to avoid damage to the gold coating.

Results

Current−Voltage Behavior of Monolayer Junctions. Figure 1 shows a typical current−voltage ($I-V$) trace for an Au-coated tip in contact with a SAM of decane thiol on Au. The

(17) (a) Paulson, S.; Helser, A.; Nardelli, M. B.; Taylor, R. M.; Falvo, M.; Superfine, R.; Washburn, S. *Science* **2000**, *290*, 1742−1744. (b) Dai, H.; Wong, E. W.; Lieber, C. M. *Science* **1996**, *272*, 523.

(18) Yano, K.; Kyogaku, M.; Kuroda, R.; Shimada, Y.; Shido, S.; Matsuda, H.; Takimoto, K.; Albrecht, O.; Eguchi, K.; Nakagiri, T. *Appl. Phys. Lett*. **1996**, *68*, 188.

(19) Klein, D.; McEuen, P. *Appl. Phys. Lett*. **1995**, *66*, 2478.

(20) Leatherman, G.; Durantini, E. N.; Gust, D.; Moore, T. A.; Moore, A. L.; Stone, S.; Zhou, Z.; Rez, P.; Liu, Y. Z.; Lindsay, S. M. *J. Phys. Chem. B* **1999**, 103, 4006−4010.

(21) Salmeron, M.; Neubauer, G.; Folch, A.; Tomitori, M.; Ogletree, D. F.; Sautet, P. *Langmuir* **1993**, *9*, 3600−3611.

(22) Lang, N. D.; Avouris, Ph. *Phys. Rev. Lett*. **2000**, 84, 358−361.

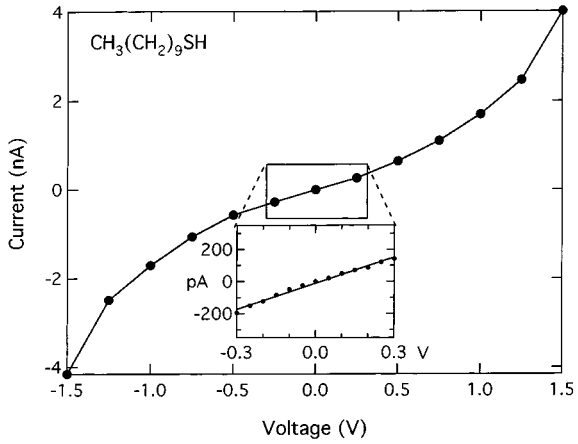

Figure 1. Current−voltage ($I-V$) characteristic for a $CH_3(CH_2)_9SH$ monolayer junction. The black line is a fit to the data using Equation 2 with $\phi = 2.2$ eV and $s = 10$ Å. Voltage shown is the voltage applied to the tip; the substrate was grounded. Tip load was 1 nN. Inset shows the approximately linear $I-V$ over ±0.3V.

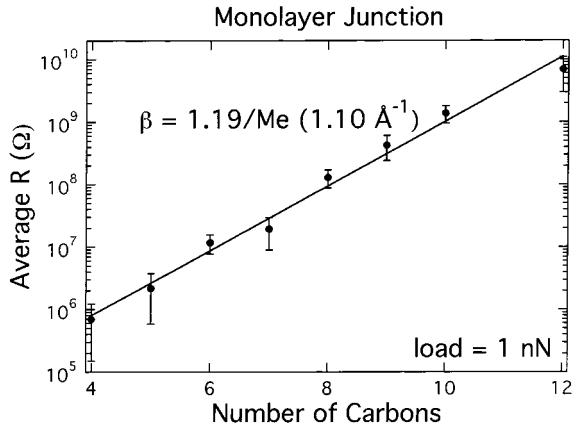

Figure 2. Semilog plot of monolayer junction resistance versus SAM thickness (number of carbons). The data were acquired with the same tip at a load of 1 nN. Each data point is the average of at least five measurements; the uncertainty is quoted as the standard deviation. The linear fit gives a β value of 1.19/CH_2, or about 1.1 Å^{-1}.

applied load to the tip microcontact was 1 nN. The trace is sigmoidal over the +1.5 to −1.5 V sweep, but is linear inside ±0.3 V. $I-V$ traces for SAMs composed of alkane thiols of different lengths all showed similar sigmoidal shapes, although the absolute currents were a strong function of chain length and tip radius.

The linear portion of the $I-V$ characteristic between ±0.3 V was used to define a junction resistance equal to 1/slope. Figure 2 shows a semilog plot of average junction resistance vs alkane thiol chain length, ranging from 4 to 12 total carbons (butyl thiol to dodecyl thiol). The entire data set was collected with the same Au-coated tip. It is clear that the resistance increases exponentially with the number of carbons in the chain, as expected for nonresonant electron tunneling. The slope of the plot gives a tunneling constant $\beta = 1.19$/carbon or ∼1.1 Å^{-1}.

Voltage excursions beyond 1.5 V typically resulted in junction breakdown,that is, a dramatic increase in current and irreversible changes to the junction properties. However, the specific breakdown voltage was also chain length dependent. Figure 3A shows typical breakdown $I-V$ curves for alkane thiols of varying chain length. It is clear from Figure 3A that the breakdown voltage increases with the number of carbons. Figure 3B is a plot of the breakdown voltage vs number of carbons. The trend is linear, consistent with a breakdown process that is field, not

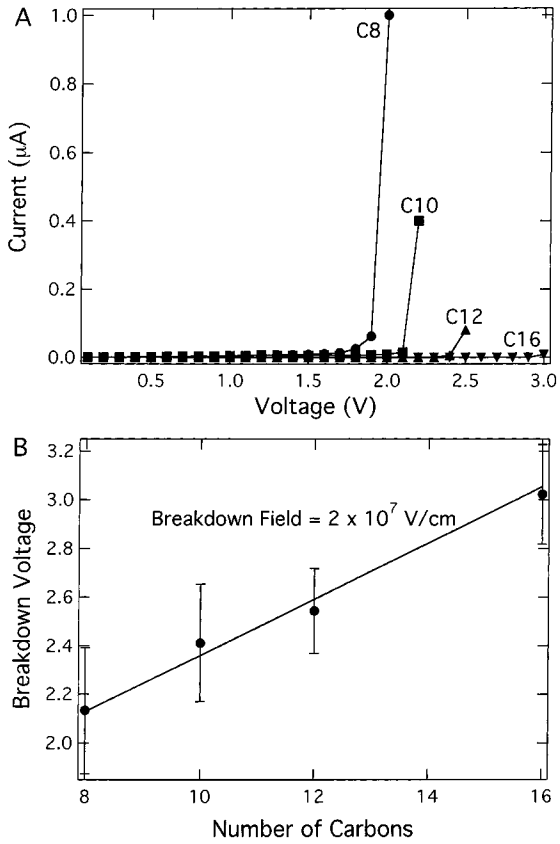

Figure 3. (A) Breakdown (BD) $I-V$ curves for SAMs of different thickness. (B) Breakdown voltage versus SAM thickness (number of carbons in the alkyl chains). Each data point is the average of at least five measurements. The straight line is a linear fit.

voltage, dependent. The slope of the linear fit corresponds to a breakdownfield of 2×10^7 V/cm, very similar to breakdown-fields observed in Hg drop junctions based on SAMs.[12b]

Load Dependence of the Junction Resistance. The junction resistance is expected to depend on the load applied to the microcontact since the SAM is compressible. Figure 4A shows the $I-V$ characteristics, obtained with one tip, for a dodecane thiol SAM as a function of load. The $I-V$s are linear at all loads between 2 and 150 nN. At loads greater than 150 nN the force is enough to push through a dodecanethiol monolayer to make Au−Au contact. In such cases, the resistances are as low as 25 Ω. At low loads less than 10 nN, load variations of a few nN result in small differences in resistance (a few %) that are within the trace-to-trace uncertainty of the measurements.

Figure 4B shows the decrease in junction resistance versus load. Interestingly, two distinct power law regimes (i.e., $R\alpha$-(load)^n) are evident in the log−log plot in the inset. Between 10 and 70 nN, $n = -0.83$. Above 70 nN the exponent n increases to −7.5.

Average junction resistances were determined as a function of alkyl chain length for three different applied loads, 2, 10, and 20 nN. Figure 5 shows average resistance versus number of carbons taken with the same tip at three different applied loads. Within experimental error, the slopes (and hence the β values) are identical.

Tip Radius Dependence of the Junction Resistance. Figure 6 displays the $I-V$ data for two tips of different radii in contact with a dodecane thiol SAM at the same applied load of 2 nN. The tip with the larger radius of curvature shows higher currents and gives a lower junction resistance, consistent with a larger microcontact area. The junction resistance for the 50 nm radius

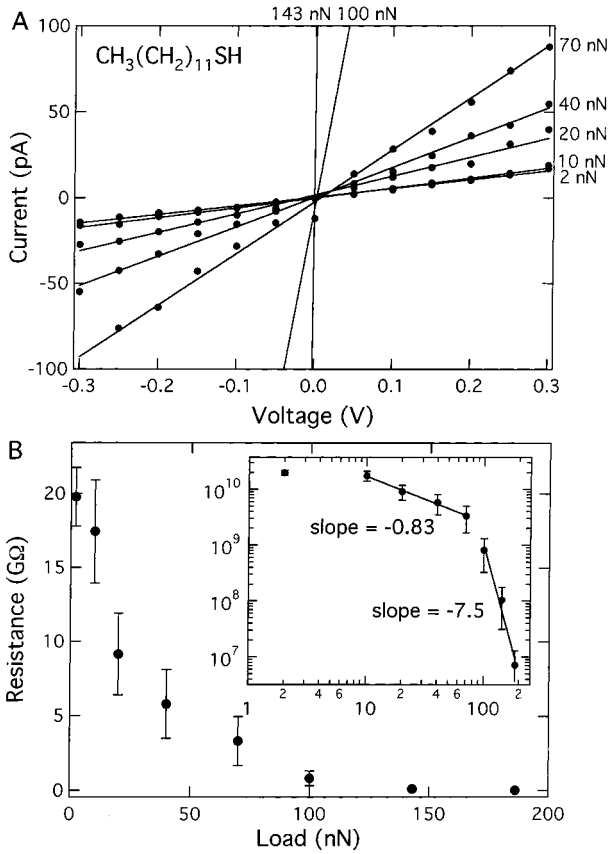

Figure 4. (A) $I-V$ characteristics of a $CH_3(CH_2)_{11}SH$ SAM as a function of applied load on the conducting tip. Traces were acquired with one tip. Solid lines are straight-line fits. (B) Junction resistance vs applied load. Resistance was taken to be the reciprocal of the slope of each straight-line fit in (A). Inset is a log−log plot showing two power law scaling regimes.

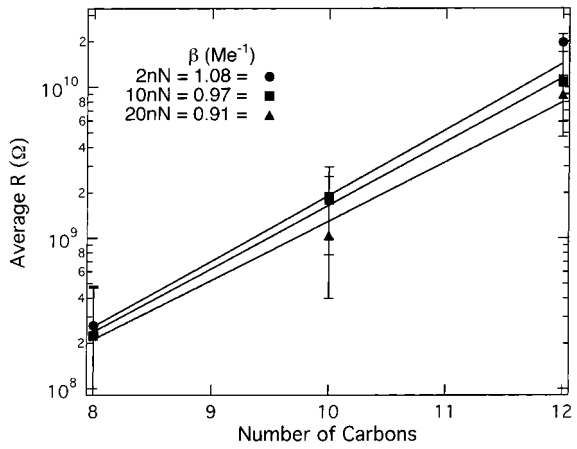

Figure 5. Semilog plot of average resistance vs SAM thickness using the same tip at three different applied loads. Straight lines are linear fits.

probe is 45 MΩ; for the 22 nm radius probe the resistance is 1.2 GΩ.

Sensitivity to Molecular Architecture. We have made a preliminary study of the dependence of the junction properties on molecular architecture. Figure 7 shows $I-V$ traces between ±50 mV for junctions based on SAMs of hexyl thiol and benzyl thiol, respectively. We estimate that the thickness of the films is comparable, approximately 6.6 ± 1.0 Å. As seen in the figure, the junction based on benzyl thiol has a resistance (0.3 MΩ) that is more than 10 times smaller than the resistance of the

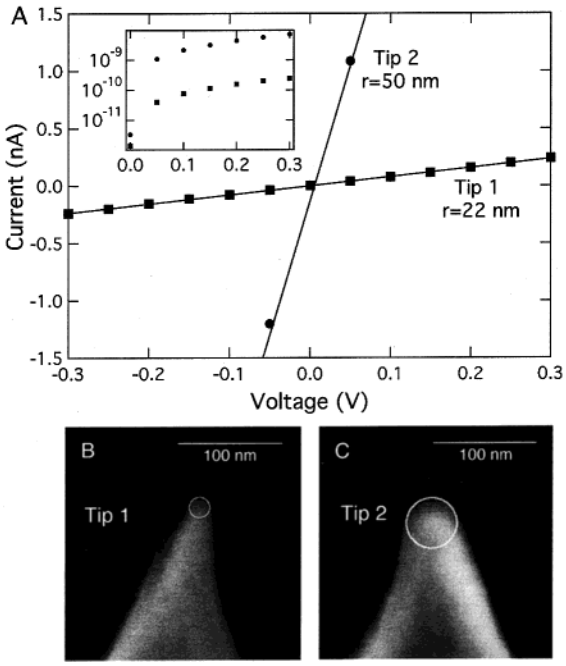

Figure 6. (A) $I-V$ characteristics of a $CH_3(CH_2)_{11}SH$ SAM acquired with sharp and blunt probes. (B) Scanning electron micrograph (SEM) of the sharp probe with a radius of 22 nm. (C) SEM of the blunt probe with a radius of 50 nm. Tip load = 2 nN.

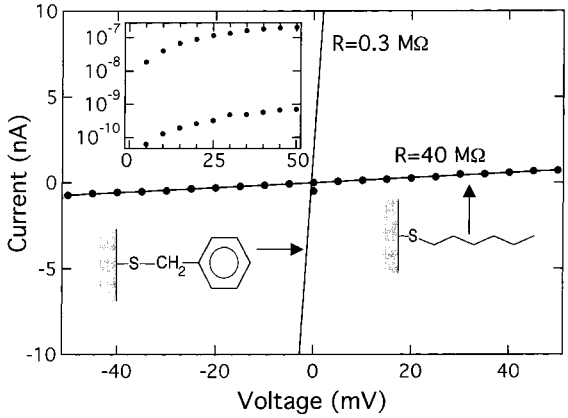

Figure 7. $I-V$ characteristics for conjugated and saturated monolayers. Lengths of the hexyl and benzyl spacers are approximately equal (6.0 ± 1.0 Å) according to bond length calculations. Data points for the benzylthiol are not visible because of the current scale. The resistances displayed are taken from the linear fits. The inset shows a semilog plot of the data from 0 to +50 mV.

hexyl thiol junctions. The data were taken with the same tip and were repeated for several samples.

Current−Voltage Behavior of Bilayer Junctions. Trace 3 in Figure 8 shows the $I-V$ characteristic of a "bilayer junction" (Scheme 2B) formed by bringing a $C_8H_{17}SH$ modified tip into contact with a $C_8H_{17}SH$ SAM on Au. Also shown for comparison are the $I-V$ characteristics for two different monolayer junctions, traces 1 and 2. All three traces were taken with the *same* Au tip so that currents are directly comparable. Trace 2 was recorded first using a bare Au probe in contact with the C8 SAM. This same tip was then modified by immersion in an ethanol solution of $C_8H_{17}SH$ for 8 h. The modified probe was then contacted to bare Au to generate trace 1 and then contacted to a $C_8H_{17}SH$ SAM to generate trace 3.

All three traces are linear over the voltage range. As expected, the bilayer junction gives by far the highest resistance, namely

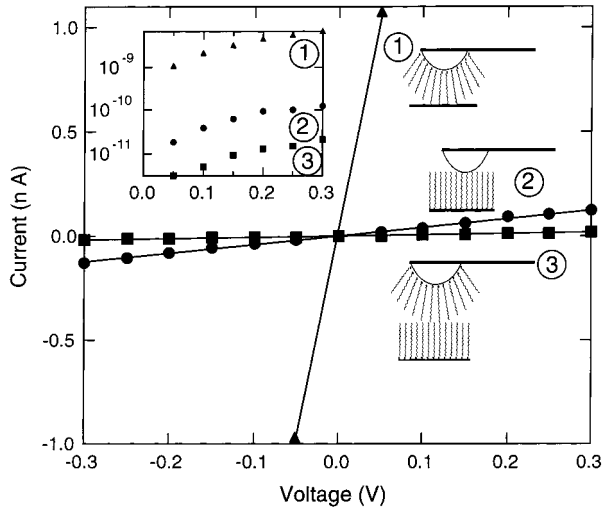

Figure 8. *I*−*V* characteristics of a bilayer junction. Trace 2 (filled circles), recorded first, shows the *I*−*V* for a bare Au tip in contact with a $CH_3(CH_2)_7SH$ SAM. Trace 1 (filled triangles) shows the *I*−*V* for this same tip, coated with a $CH_3(CH_2)_7SH$ SAM, contacted to a clean Au surface. Trace 3 (filled squares) shows this coated tip in contact with an $CH_3(CH_2)_7SH$ SAM, creating the bilayer architecture. The inset shows a semilog plot from 0 to +0.3 V.

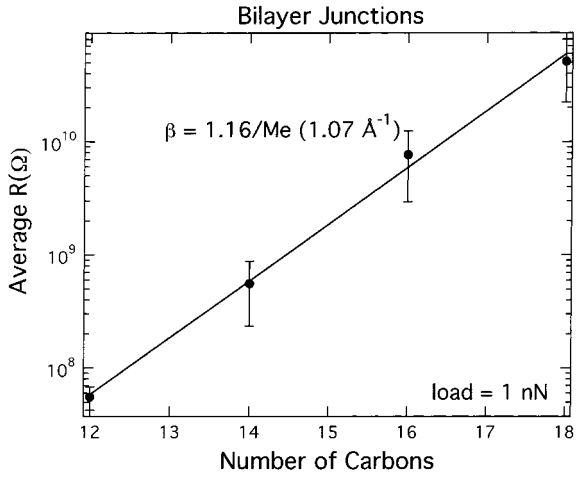

Figure 9. Semilog plot of bilayer junction resistance vs SAM thickness (number of carbons). Each data point is the average at least 6 measurements. The uncertainty bars represent the standard deviations. The number of carbons includes eight for the tip SAM and from 4 to 10 for the surface SAM. The linear fit gives a β value of 1.16/CH_2, or about 1.1 Å^{-1}. The data were acquired with the same tip at 1 nN load.

20 GΩ. The trace 1 and trace 2 junction resistances are 0.2 and 2 GΩ, respectively, implying that the molecular configurations in the junctions are not equivalent.

Figure 9 shows a semilog plot of the average resistance for a bilayer junction as a function of number of carbons, or bilayer thickness. "Number of carbons" was computed by adding the carbon chain length for the tip-bound molecules to the chain length for the substrate-bound molecules. As Scheme 2B indicates, these experiments were accomplished by bringing the same C8-modified tip into contact with SAMs having different chain lengths. The Figure 9 plot is linear, indicating exponential dependence of the junction resistance on the bilayer thickness. Furthermore, we find from this plot that $\beta = 1.07$ Å^{-1}, which is remarkably similar to the β obtained for monolayer junctions (1.1 Å^{-1}), Figure 2.

Discussion

Transport Mechanism. The mechanism of transport through these metal−molecule−metal junctions at voltages less than breakdown is nonresonant tunneling, based on both the *I*−*V* characteristics (Figure 1) and the thickness dependence of the junction resistance (Figure 2). In Figure 1 we have compared our experimental *I*−*V* data for an Au−$CH_3(CH_2)_9SH$−Au junction to a simple model for coherent nonresonant tunneling in planar metal−insulator−metal junctions:[23]

$$I = I_0\{\bar{\phi}\exp[-A\bar{\phi}^{1/2}s] - (\bar{\phi} + eV)\exp[-A(\bar{\phi} + eV)^{1/2}s]\} \quad (2)$$

where *I* is the current, *V* is the applied potential, *s* is the insulator thickness, I_0 is a constant, $A = 2(2m)^{1/2}/\hbar$ where *m* is the electron mass, and $\bar{\phi}$ is the mean height of the potential barrier associated with the insulator. To fit the *I*−*V* data in Figure 1, I_0, $\bar{\phi}$, and *s* were treated as adjustable parameters. It is evident that good agreement between the data and the model is obtained with $\bar{\phi}$ = 2.2 eV and *s* = 10 Å. The 10 Å value for the insulator thickness is reasonable for a $CH_3(CH_2)_9SH$ SAM.[24] In principle, the value of $\bar{\phi}$ should be a qualitative measure of the position of the Fermi level (E_F) within the HOMO−LUMO gap. The key point that we emphasize now is that eq 2, which is based on a very simple model of nonresonant tunneling, gives a reasonable description of our observed *I*−*V* data.

It can be shown that for small voltages eq 2 reduces to[23]

$$I = I_0'\bar{\phi}^{1/2}V\exp[-A\bar{\phi}^{1/2}s] = I_0'\bar{\phi}^{1/2}V\exp[-\beta s] \quad (3)$$

where the structure dependent prefactor $\beta = A\bar{\phi}^{1/2}$ has units of 1/length. Equation 3 shows that *I* is directly proportional to *V* and also depends exponentially on the barrier width, *s*. Over small voltage ranges, ±0.3 V, the measured *I*−*V* characteristics for the SAM junctions are indeed linear, Figure 1, and Figure 2 shows that the junction resistances increase exponentially with SAM thickness. From the slope of the semilog plot in Figure 2, we determine the prefactor β to be 1.19 per −CH_2− or ∼1.1 Å^{-1}.[25] This value is in good agreement with β values determined for alkane chains in STM studies (1.2 Å^{-1}),[9a] Hg drop junctions (0.9 Å^{-1}),[12] and electrochemical experiments (∼1 Å^{-1}).[8e] The fact that we are able to fit the junction characteristics with a simple model for transport through a metal−insulator−metal junction and that we obtain reasonable values for β supports the conclusion that the transport mechanism is coherent nonresonant tunneling. Our results also suggest that formation of metal−molecule−metal junctions using conducting AFM tips is a reliable and useful approach to determining the distance dependence of electron tunneling in molecules.

Load Dependence and Contact Area. The ability to vary the load applied to the tip−SAM contact is a unique characteristic of our junctions and allows us to probe the effect of mechanical deformation of the SAM on the junction resistance. Figure 4 shows that over a range of ∼150 nN, resistance of the junction decreases as load increases. This is expected since increasing the load should (1) increase the tip−SAM contact area and (2) compress the SAM, making the tunneling barrier thinner. The log−log plot in Figure 4B of resistance versus load shows two distinct scaling regimes. Between 10 and 70 nN

(23) Simmons, J. G. *J. Appl. Phys*. **1963**, 34, 1793−1803.
(24) Troughton, E. B.; Bain, C. D.; Whitesides, G. M.; Nuzzo, R. G.; Allara, D. L.; Porter, M. D. *Langmuir* **1988**, *4*, 365−385.
(25) In converting the units of β from (per CH_2) to Å^{-1} we have estimated that on average each −CH_2− group increases the SAM thickness by 1.1 Å.

resistance scales as $(\text{load})^{-0.83}$. At loads greater than 90 nN, we observe a much steeper dependence, resistance $\propto (\text{load})^{-7.5}$. Extrapolation of the linear fits indicates that the transition between the two regimes occurs at just over 70 nN.

The power law exponent in the low-load regime is reasonably close to the expected scaling based on Hertzian contact mechanics. The Hertz model[26] predicts that the tip−SAM contact area should scale as $(\text{load})^{2/3}$, meaning resistance, which is inversely proportional to the contact area, could be expected to scale as $(\text{load})^{-0.67}$. The fact that a stronger dependence is observed may reflect the fact that the junction resistance does not only depend on the tip−SAM contact area but also the extent of SAM compression.

We hypothesize that the scaling transition at ∼70 nN corresponds to an abrupt change in the structure of the compressed SAM. Indeed, previous AFM imaging studies of alkane thiol SAMs have shown that abrupt changes in lattice symmetry are observed upon exceeding a critical load on the tip.[27] Salmeron and co-workers[27b] reported that, at tip pressures less than 1 GPa, the $(\sqrt{3} \times \sqrt{3})R30°$ lattice characteristic of alkane thiols SAMs is observed but that, as tip pressure is increased, the resolution degrades. Above a critical pressure of ∼2.3 GPa the images revealed the underlying Au(111) lattice. These workers conjectured that increased pressure produced disorder in the SAM that degraded resolution, and above the critical pressure it appeared that the tip displaced the thiol molecules. Monte Carlo calculations by Siepmann[28] indicated that gauche defects are induced in alkane thiol SAMs upon increasing pressure, supporting the idea of pressure-induced disorder. The data shown in Figure 4 were taken with a 50 nm radius probe, which means our 70 nN critical load corresponds to ∼5 GPa. The detailed relationship between the imaging studies and our resistance versus load measurements remains to be determined in further experiments. However, it does seem plausible that the two power law regimes in Figure 4B are due to load-induced structural transitions in the SAM, perhaps introduction of chain kinks at loads less than 70 nN and then actual displacement of molecules above that load. Resistance measurements as a function of load may prove to be a sensitive and general method for investigating structural deformations in monolayer films.

During our $I-V$ measurements there is a small "electrostatic load" on the junction in addition to the mechanical load applied by the cantilever. This electrostatic force arises from the attraction between the tip and substrate as the voltage on the tip is increased. Approximating the tip as a sphere of radius R, this electrostatic or capacitance force can be estimated by[29]

$$F(z) = \pi\epsilon V^2\left[\frac{R^2}{z(z+R)}\right] \qquad (4)$$

where z is the thickness of the intervening dielectric, ϵ is the permittivity of the dielectric, and V is the applied voltage. At 1 V applied tip bias, the calculated electrostatic load is ∼1 nN. At 0.3 V, which was the maximum voltage for many of our measurements, the load is ∼0.1 nN. Inspection of Figure 4 shows that the junction resistance is relatively insensitive to *small* load variations on the order of 1 nN. This is also seen in Figure 5, which shows that the β value varies by only about 20% over applied loads ranging from 2 to 20 nN. Thus, it does not appear that the electrostatic force between the tip and substrate significantly impacts our measurements.

An explanation for why small load variations of 1 nN or less do not affect the junction characteristics, at low applied loads in particular, is that there is substantial adhesion between the tip and the SAM. Measured tip−SAM pull-off forces are 10−15 nN, depending on tip radius, meaning that even at zero *applied* mechanical load, there is an effective 10−15 nN load on the junction. We estimate that a 1 nN variation in applied load results in a 3% change in the junction contact area, and thus a small change in resistance.[30]

We can also estimate the contact area using contact mechanics equations. For a tip with $R = 50$ nm placed in contact with the SAM at an applied load of 1 nN, we calculate a 15 nm^2 area.[30] On the basis of a full alkane thiol coverage of 9×10^{-10} mol/cm^2 (5 molecules/nm^2), the junction involves approximately 75 molecules.[31]

Junction Breakdown. The data in Figure 3A show that breakdown (BD) occurs at a critical field strength of 2×10^7 V/cm (∼0.2 V/CH_2) for SAMs of all thicknesses, which is in the range of reported BD strengths for bulk polyethylene ($(0.8-8) \times 10^7$ V/cm).[32] If all of the voltage applied to the junction were dropped *at the contacts*, one would expect that the BD voltage would be the same for all SAMs, that is, it would be independent of SAM thickness. Because this is not the case, at least some of the voltage is dropped across the molecule, and the molecule supports an internal field (see Scheme 1B).

The load due to electrostatic attraction of the tip to the substrate at BD voltages (∼1.5 V) is only a few nN which is well below the loads known to cause collapse of crystalline order in SAMs.[27] Thus, we think it is unlikely that BD is due to mechanical collapse of our junctions. BD is more likely caused by an electronic process. However, we are not sure at this time whether BD involves electronic processes in the molecule or at the molecule−metal interfaces. In an extensive investigation of BD in Hg/SAM/Ag junctions, Whitesides et al. also concluded that BD cannot simply be attributed to mechanical collapse of their junctions, but an electronic mechanism was not offered.[12b]

Molecular Architecture and Bilayer Junctions. Figure 7 is a demonstration that our junctions are sensitive to molecular architecture. We have found that the resistance of junctions based on benzyl thiol SAMs are more than 10 times smaller than junctions based on an alkane thiol SAM of comparable length. Because $E_{\text{HOMO-LUMO}}$ of the phenyl ring is ∼4 eV and $E_{\text{HOMO-LUMO}}$ of the alkyl chain is ∼8 eV, the smaller resistance for benzyl thiol is expected,[1−4] although detailed calculations of the junction transport properties are required to understand these results quantitatively.

The ability to measure the junction resistance with molecules chemisorbed to the tip is important because it offers the

(26) Johnson, K. L. *Contact Mechanics*; Cambridge University Press: 1985, 84−106.

(27) (a) Touzov, I.; Gorman, C. B. *J. Phys. Chem. B* **1997**, 101, 5263. (b) Lio, A.; Morant, C.; Ogletree, D. F.; Salmeron, M. *J. Phys. Chem. B* **1997**, 101, 4767−4773.

(28) Siepmann, J. I.; McDonald, I. R. *Phys. Rev. Lett.* **1993**, 70, 453.

(29) Hudlet, S.; Saint Jean, M.; Guthmann, C.; Berger, J. *Eur. Phys. J. B* **1998**, 2, 5−10.

(30) Radius, a, of the tip−SAM contact is given by Hertzian mechanics as, $a = (RF_{\text{applied}}/K)^{1/3}$ (see ref 26), where R is the radius of the tip, F_{applied} is the load on the microcontact, and K is an elastic modulus. Taking F_{applied} to be 16 nN (the sum of the 15 nN adhesive or pull-off load and the 1 nN applied load), $R = 50$ nm, and $K = 77$ GPa for Au (ignoring the mechanical properties of the SAM), gives $a = 2.2$ nm, corresponding to a contact area of 15 nm^2. Increasing F_{applied} to 17 nN increases the estimated contact area by 3% to 15.5 nm^2.

(31) The number of molecules involved in charge transport may be greater than 75 if a significant portion of the measured current results from electrons that tunnel between the tip and the substrate just outside the perimeter of the microcontact. Further studies are needed to pinpoint the effective cross-sectional area available for electron tunneling in the junction.

(32) (a) Ieda, M.; Nagao, M.; Sawa, G. *IEEE Conf. On Dielectr. Mater., Meas., and Appl.* **1979**, 177, 185−188. (b) Whitehead, S. *Dielectric Breakdown of Solids*, Oxford University Press: Oxford, U.K., 1953.

opportunity to probe the effects of functional group interactions between proximal monolayers. In Figure 9, we show that the β value for these bilayer junctions is identical, within experimental error, to the β value obtained for monolayer junctions. That is not surprising because in these bilayer experiments only the chain lengths of the molecules on the substrate SAM were varied; the SAM on the tip was always $C_8H_{17}SH$. If the chain length of the tip SAM is varied instead, we have preliminary evidence that the β value is not the same as that of the monolayer junction.[33] This may be because the organization of the alkane thiols on the tip is more defective.

In summary, we have shown that CP-AFM provides a useful approach to the formation of metal−molecule−metal junctions and the study of electron transfer in molecules that can be assembled on conducting substrates. The junction $I-V$ characteristics are sensitive to the applied load on the tip contact, the tip radius, the HOMO−LUMO gap of the SAM molecules, and the presence of chemisorbed molecules on the tip. We have been able to determine β values reproducibly for alkane thiol SAMs in both monolayer and bilayer configurations. Further studies that probe the role of functional groups and applied load on the junction $I-V$ characteristics appear to be promising avenues.

Acknowledgment. C.D.F. thanks the National Science Foundation (DMR No. 9624154) and the David and Lucile Packard Foundation for supporting this work.

JA0101532

(33) Wold, D. J.; Frisbie, C. D., unpublished results.